arXiv:1209.0920v1 [cond-mat.mes-hall] 5 Sep 2012

Optical measurement and modeling of interactions between two hole or two electron spins in coupled InAs quantum dots

A. Greilich[1,2], Ş. C. Bădescu[1,3], D. Kim[1,4], A. S. Bracker[1], D. Gammon[1]
[1] *Naval Research Laboratory, Washington, DC 20375, USA*
[2] *Technische Univerität Dortmund, 44221 Dortmund, Germany*
[3] *Air Force Research Laboratory, Wright-Patterson AFB, OH 45433, USA*
[4] *Harvard University, Cambridge, MA 02138, USA*

(Dated: September 6, 2012)

Two electron spins in quantum dots coupled through coherent tunneling are generally acknowledged to approximately obey Heisenberg isotropic exchange. This has not been established for two holes. Here we obtain the spectrum of two holes and of two electrons in two vertically stacked self-assembled InAs quantum dots using optical spectroscopy as a function of electric and magnetic fields. We find the exchange to be dominantly isotropic for both systems, with observed anticrossing singularities that can only be explained by asymmetric mixing. The latter arises from spin-orbit and Zeeman interactions combined with spatial asymmetries. Such asymmetric contributions to the isotropic Hamiltonian for electrons are of the order of a few percent while those for holes are an order of magnitude larger.

PACS numbers: 71.70.Ej, 71.70.Gm, 78.55.Cr, 78.67.Hc

The exchange interaction between the spins in two quantum dots (QDs) leads to entanglement and to the opportunity of quantum information processing [1]. Electron spin qubits have been studied in great detail, but recently hole spins have received special attention [2, 3] because of their reduced hyperfine interaction with the nuclear spin reservoir [4–7]. Now, for inter-QD entanglement, the nature of the exchange interaction is of central importance, both for quantum gates and for decoherence of two-qubit states.

The symmetry of this interaction is often assumed to be the Heisenberg isotropic exchange, $J\boldsymbol{\sigma}_1 \cdot \boldsymbol{\sigma}_2$. As a result, the eigenstates of two spins in two quantum dots form singlet and triplet spin states separated by the exchange energy, J. This model is very important, conceptually [1] and for interpretations of complex experimental spectra [8], and has been used widely in magnetism, quantum computing, molecular and quantum dot structures. It has been shown that for two bound electrons the isotropic Heisenberg interaction captures almost all of the physics and it requires only small asymmetric exchange terms that couple singlets and triplets [9–14].

These small singlet-triplet mixings are important in spin relaxation in bulk GaAs [15]. In QDs, they require solutions to remove their effects on the fidelity of two-qubit gates [16, 17].

In contrast to electron spins, hole spins are extremely anisotropic, for example, in their g-factor [18] and in their hyperfine interaction [19]. This anisotropy arises from the strong spin-orbit character of the valence band. Counterintuitively, we find that isotropic hole-hole exchange between two self-assembled InAs QDs is in fact a good starting point [20]. This surprising result was predicted by theory, which demonstrated that in the absence of heavy hole -light hole mixing, exchange between two hole spins in two QDs should be isotropic, just like two electron spins [21]. Now we find that substantial asymmetric contributions arising from spin-orbit interactions and inhomogeneous Zeeman interactions are necessary to understand the measured $2h$ energy levels.

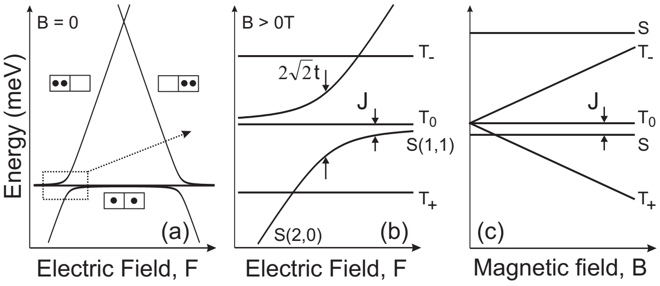

FIG. 1. (a) Hund-Mulliken model for two-spin configuration at zero B. (b) F dependence at fixed B for a symmetric case, Eq. (2). (c) B dependence at fixed F (marked by arrows with J in (b)).

The asymmetric contributions are often overlooked in spectroscopy due to their small perturbations to QD energy levels, where the energies are dominated by the isotropic exchange. In this paper we present an optical study to identify and measure asymmetric contributions to the interaction between two holes ($2h$) and also between two electrons ($2e$) in two tunnel-coupled QDs. We use individual pairs of vertically stacked self-assembled InAs/GaAs QDs separated by a thin tunnel barrier with a thickness d. Two types of samples were developed using a Schottky diode grown by molecular beam epitaxy, one for $2h$ [3] and one for $2e$ [22]. The width and height of the tunnel barriers were selected in a way that allowed us to achieve similar values of singlet-triplet splitting for both cases ($J \approx 100\,\mu$eV) [23]. Electric (F) and magnetic (B)

fields were applied longitudinally along the stacking z-axis in the Faraday geometry and are used to balance the dominant isotropic exchange and to bring the energy levels to resonance displaying their mixings. Measurements were done at 5 K using photoluminescence with a spectral resolution limited by the spectrometer of $\sim 15\,\mu$eV, and laser transmission spectroscopy with a resolution determined by the linewidth ($\sim 6\,\mu$eV for holes and $\sim 3\,\mu$eV for electrons).

The Heisenberg exchange can be treated within the Hund-Mulliken model [24, 25]. The natural spin state basis is three triplets: $T_0 = (\uparrow,\downarrow)_{T_0}$, $T_+ = (\uparrow,\uparrow)_{T_+}$, $T_- = (\downarrow,\downarrow)_{T_-}$ and three singlets: $S_{(2,0)} = (\uparrow\downarrow,0)_S$, $S_{(1,1)} = (\uparrow,\downarrow)_S$, and $S_{(0,2)} = (0,\uparrow\downarrow)_S$. The individual spin projections are either the electron spin $\pm 1/2$ or hole pseudo-spin $\pm 1/2$. The singlet states are coupled together and shifted in energy by spin conserving tunneling (t) between the two QDs, but because of spin blocking, the triplet states are not affected. The Hamiltonian within the singlet basis is given by:

$$\begin{array}{c} \begin{array}{ccc} (\uparrow\downarrow,0)_S & (\uparrow,\downarrow)_S & (0,\uparrow\downarrow)_S \end{array} \\ \begin{pmatrix} Fd+U & -\sqrt{2}t & 0 \\ -\sqrt{2}t & 0 & -\sqrt{2}t \\ 0 & -\sqrt{2}t & -Fd+U \end{pmatrix} \end{array} \tag{1}$$

The potential (U) is the Coulomb energy required to move the two charges from separate QDs to the same QD. The relative energy between QDs separated by d is controlled via F. In Fig. 1(a), the resulting levels of the singlets show anticrossings. The lowest energy singlet state is $S = aS_{(2,0)} + bS_{(1,1)} + cS_{(0,2)}$. In Fig. 1(b) and hereafter we focus on one of the anticrossings, for which $c = 0$. The isotropic exchange interaction J is defined as the splitting between T_0 and the lowest singlet with the spin Hamiltonian $J\boldsymbol{\sigma}_1 \cdot \boldsymbol{\sigma}_2$, with $J = J(F,U,t)$.

To fully probe and engineer the spin states of the two QDs we also need, in addition to F, a magnetic field. The simplest Hamiltonian consists of isotropic exchange and an average Zeeman interaction,

$$H = J\boldsymbol{\sigma}_1 \cdot \boldsymbol{\sigma}_2 + \boldsymbol{\beta}^{ext} \cdot (\boldsymbol{\sigma}_1 + \boldsymbol{\sigma}_2) \tag{2}$$

The Zeeman term $\boldsymbol{\beta}^{ext} = (g_{11} + g_{22})\mu_B \boldsymbol{B}/2$ splits the T_+ and T_- lines, but preserves the spin states. In Fig. 1(c) the energies are calculated as a function of B with F held constant. We find experimentally that this symmetric approximation is fairly good for two electrons but less so for two holes.

Calculated transitions from the $2h$ levels to the charged exciton levels (X^{2+}) are shown within the symmetric approximation in Fig. 2(a). Here we show the dependence on B, holding F constant. The exciton states have been described previously [8, 25]. The corresponding transition spectrum is shown in Fig. 2(b). At zero B the transition spectrum shows a doublet with a splitting given by the exchange J, which then separates into four transition lines with increasing B. Transitions involving S are non-degenerate at finite B, but those involving T_0, $T_\pm$ remain two-fold degenerate – in the absence of asymmetry.

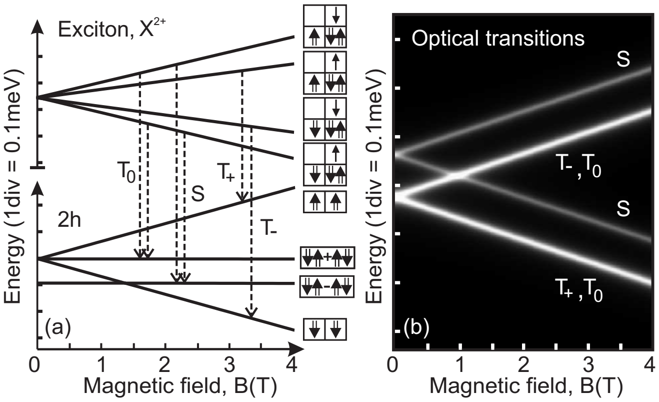

FIG. 2. (a) Calculated B dependence for the excited and ground states for the $2h$ in symmetric case. Transitions are labeled by final state. (b) calculation of the transition spectrum for the B dependence of X^{2+} using the parameters: $g_e = -0.46$, $g_{h,1} = g_{h,2} = 1.1$, $t = -115\,\mu$eV, $U = 10\,$meV. The diamagnetic shift is not taken into account.

In contrast to the symmetric calculation of Fig. 2(b), the measured $2h$ spectrum appears much more complex as shown in Fig. 3(a). In addition to substantial line splittings observed in the triplet optical transitions that grow with increasing B, there are now anticrossings with magnitudes of $26\,\mu$eV at $B = 1.5\,$T. These anticrossings cannot be captured by a symmetric hamiltonian and require off-diagonal matrix elements that describe coupling between S and T. We will call them "spin-flip" anticrossings. We have also measured the $2h$ optical spectrum as a function of F at fixed B. The complex pattern of anticrossings observed in the data of Fig. 3(d) arises from spin-conserving anticrossings of both the $2h$ and the exciton states as discussed previously [25] combined with the smaller spin-flip anticrossings. All of these features can be explained with natural extensions of the symmetric Hamiltonian Eq. (2) as we discuss below. As a result we obtain the fitted optical transition spectrum shown in Figs. 3(b) and 3(e), and calculate the corresponding $2h$ energy levels in Figs. 3(c) and 3(f). A comparison of these results and the symmetric calculations of Fig. 1 is additional evidence that asymmetric contributions are important.

The $2e$ optical spectrum found in a manner similar to that of Fig. 3(a) gives a much smaller spin-orbit contribution than for the $2h$ case. In fact it was necessary to use the higher resolution of laser spectroscopy to resolve the additional structure [22]. The magnitude ($4\,\mu$eV) of the spin-flip anticrossing was 4% that of the symmetric exchange ($100\,\mu$eV) and 1% that of the spin-conserving tunneling anticrossing. In addition, the splitting in the triplet optical transition at high fields ($4\,\mu$eV at 4 T) due

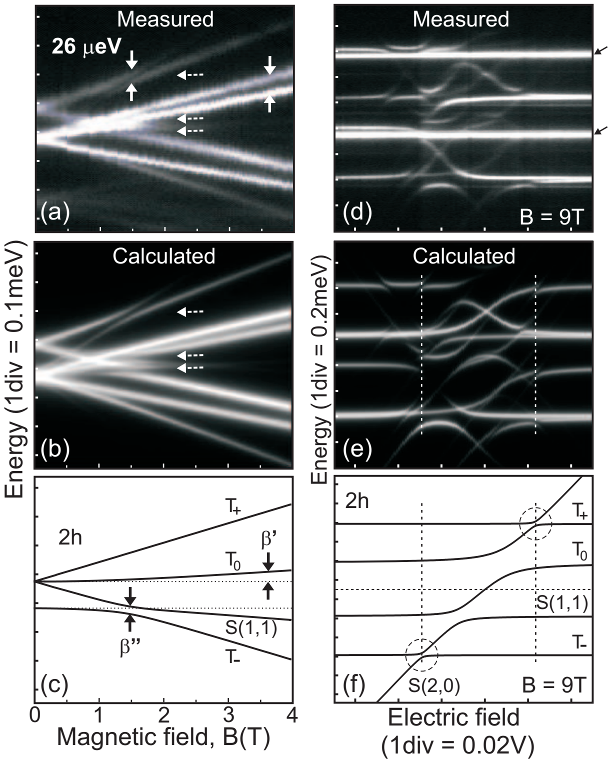

FIG. 3. (a) measured and (b) calculated transition spectra of B dependence for the X^{2+}. $g_{h,1} = 1.85$, $g_{h,2} = 0.78$, $g_e = -0.46$, $g_{h,12} = 0.14$, $t = -115\,\mu$eV, $\gamma_{12} = 24\mu$eV, $\Delta\gamma \sim 5\,\mu$eV. (a) and (b) Three signatures of AC are marked by dashed horizontal arrows. A diamagnetic shift of $11.6\,\mu\text{eV/T}^2$ is subtracted in (a). (c) Calculated $2h$ energy levels with ground state S/T_- AC of 26μeV. (d) measured and (e) calculated transition spectra of F dependence for $B = 9\,$T. (small black arrows on the right of panel (d) mark a transition spectra of X$^+$.) (f) Ground state energy levels as a function of bias. Circles mark the spin-flip ACs. Vertical lines mark the position of ACs in transition spectra of Fig. 3(d) and 3(e).

to g-factor inhomogeneity was small.

In the data modeling shown in Fig. 3 we have generalized the symmetric spin Hamiltonian of Eq. (2) to include spin coupling terms as follows. The spin interaction of holes (or electrons) again is included with interaction terms, $\boldsymbol{\beta}_1^{tot} \cdot \boldsymbol{\sigma}_1 + \boldsymbol{\beta}_2^{tot} \cdot \boldsymbol{\sigma}_2$ acting on each spin. The fields now include not only the external B but also the internal relativistic magnetic fields arising from the spin-orbit interaction $\boldsymbol{\beta}_i^{tot} = \boldsymbol{\beta}_i^{ext} + \boldsymbol{\beta}_i^{so}$. We could also include the Overhauser fields due to the hyperfine interaction with nuclear spins, in a similar way to Ref. [14], but this is expected to be small here. After integrating over the orbital degrees of freedom and including the isotropic exchange we obtain the general spin Hamiltonian for two spins in two QDs:

$$H = J\boldsymbol{\sigma}_1 \cdot \boldsymbol{\sigma}_2 + \boldsymbol{\beta} \cdot (\boldsymbol{\sigma}_1 + \boldsymbol{\sigma}_2) + \boldsymbol{\beta}' \cdot (\boldsymbol{\sigma}_1 - \boldsymbol{\sigma}_2) + \boldsymbol{\beta}'' \cdot (\boldsymbol{\sigma}_1 \times \boldsymbol{\sigma}_2) \tag{3}$$

In general each of the interaction terms can depend on both external and internal fields. In our case, the strong axis of the QDs and also the external B are along the z-axis, $\boldsymbol{B} = B\hat{\boldsymbol{z}}$. The QDs are also stacked along the z-axis, and we take any lateral asymmetry (e.g. an offset between the centers of the QDs) to lie along the x-axis. As a result the internal field $\boldsymbol{\beta}^{so} = \gamma\hat{\boldsymbol{x}}$. With these Zeeman and spin-orbit fields the parameters in Eq. (3) can be written:

$$\begin{aligned} \boldsymbol{\beta} &= 1/2\mu_B B \Sigma g \hat{\boldsymbol{z}} + \Sigma\gamma\hat{\boldsymbol{x}} \\ \boldsymbol{\beta}' &= 1/2\mu_B B (a g_{12} + b\Delta g)\hat{\boldsymbol{z}} \\ \boldsymbol{\beta}'' &= (a\gamma_{12} + b\Delta\gamma)\hat{\boldsymbol{x}}. \end{aligned}$$

The Zeeman interaction with the external B is determined by the matrix elements of the coordinate-dependent g-factor $g(r)$ over the two QDs: $\Sigma g = (g_{11} + g_{22})$, $\Delta g = (g_{11} - g_{22})$ and $g_{12} = \langle 1|g(r)|2\rangle$. Likewise, the spin-orbit field leads to mixing terms given by matrix elements of γ. The linear superposition $aS_{(2,0)} + bS_{(1,1)}$ gives a contribution of γ_{12} and $\Delta\gamma$, which is determined by measuring it's dependence on F.

We can also write the Hamiltonian of Eq. (3) in a matrix form within the singlet/triplet spin basis that shows explicitly how the states are mixed, and permits convenient fitting to the data.

$$\begin{array}{c} \begin{array}{ccccc} (\uparrow\downarrow,0)_S & (\uparrow,\downarrow)_S & (\uparrow,\downarrow)_{T_0} & (\uparrow,\uparrow)_{T_+} & (\downarrow,\downarrow)_{T_-} \end{array} \\ \begin{pmatrix} Fd+U & -\sqrt{2}t & \alpha\sqrt{2}g_{12} & \gamma_{12} & -\gamma_{12} \\ -\sqrt{2}t & 0 & \alpha\Delta g & -\Delta\gamma & \Delta\gamma \\ \alpha\sqrt{2}g_{12} & \alpha\Delta g & 0 & \Sigma\gamma & \Sigma\gamma \\ \gamma_{12} & -\Delta\gamma & \Sigma\gamma & \alpha\Sigma g & 0 \\ -\gamma_{12} & \Delta\gamma & \Sigma\gamma & 0 & -\alpha\Sigma g \end{pmatrix} \end{array} \tag{4}$$

Using Eq. (4) we were able to get good fits to the data as shown in Fig. 3. We obtain the coupling parameters $(\Sigma g, \Delta g, g_{12}) = (2.63, 1.07, 0.14)$, and $(\Sigma\gamma, \Delta\gamma, \gamma_{12}) = (0, 5, 24)\,\mu$eV.

The diagonal terms correspond to the symmetric Hamiltonian of Eq. (2). The new off-diagonal terms lead to the observed energy splittings and anticrossings in the spectra. The phenomenological Zeeman and spin-orbit parameters, g_{ij} and γ_{ij}, have useful physical interpretations. First, the term with Δg is manifestly the difference in g-factors between the two QDs, and likely arises from the difference in size and indium concentration between the two QDs. This parameter is larger for holes than for electrons in part because the larger effective mass of the hole makes them more localized and more sensitive to differences of the QDs. The term with g_{12} physically arises from the difference in g-factor between the barrier and the QDs, which leads to the $\uparrow$ and $\downarrow$ spins-tunneling at different rates [26]. This terms breaks the spin symmetry and mixes S and T_0. At sufficiently high fields the eigenstates become $(\uparrow,\downarrow)$ and $(\downarrow,\uparrow)$, instead of $(\uparrow,\downarrow)_S$ and $(\uparrow,\downarrow)_{T_0}$ [27].

These off-diagonal Zeeman terms effectively push the S and T_0 energies apart as a function of B as seen in Fig. 3(c), arrows on the right. This is measured directly in the optical spectrum by the splitting in the triplet transitions that grows with B. This splitting is potentially important because it enables resonant optical control and measurement of each of the spin states separately. Recent studies have demonstrated optical quantum control of coherent superposition of the T_0 and S for $2e$ [22, 28] and $2h$ [3] states. New opportunities in control and measurement may be possible with further increases of the triplet splitting that arises from differences in g-factors. For example, if the S and T_0 states are used as an optically controlled qubit, the T_- and T_+ transitions could provide cycling transitions for readout, analogous to what has been done with a single electron qubit system [29].

The result of the spin-orbit field is similar but with an important difference. The spin-orbit field acting orthogonal to $\hat{\mathbf{z}}$ has the effect of partially rotating $\uparrow$ to $\downarrow$, and vice versa. In particular, the term γ_{12}, which couples $(\uparrow\downarrow, 0)_S \leftrightarrow (\uparrow,\uparrow)_{T_-}$, can be viewed as spin-flip tunneling. It is analogous to the spin conserving tunneling term (t), which couples $(\uparrow\downarrow, 0)_S \leftrightarrow (\uparrow,\downarrow)_S$. The γ_{12} term along with the $\Delta\gamma$ term have the effect of mixing the S state with the T_- and T_+ triplet states, and leads to the anticrossing observed in Fig. 3(c). Quantum control of two holes in this system could thus be obtained with electrostatic gates in a way analogous to Taylor *et al.* [30], however, instead of hyperfine coupling, the much larger spin-orbit interaction could be used.

The term $\Sigma\gamma$ couples T_0 with the T_+ and T_- triplets. It can be measured as a splitting of the triplet line at zero B. Any zero-field splitting of the triplet energies was found to be less than our resolution of $15\,\mu$eV for the $2h$ transitions, and so we took this parameter to be zero [31]. We note that in a separate study there is evidence for a very small splitting of $\sim 8\,\mu$eV in a similar sample from coherent measurements in the time domain [3].

Microscopically, the β^{so} field arises from spin-orbit interactions combined with spatial asymmetry (e.g. the lateral displacement of the two stacked QDs). It does not couple the states directly but rather results indirectly from coupling with excited states [32]. More generally, the magnitude of asymmetric exchange will depend on the width of the tunneling barrier and on the magnitude of spatial asymmetry (e.g. misalignment of the QDs).

Here we have found that a symmetric spin Hamiltonian based on the isotropic Heisenberg exchange interaction can be generalized to treat the $2h$ as well as the $2e$ spectrum in tunnel-coupled QDs using phenomenological off-diagonal Zeeman and spin-orbit parameters.

[1] D. Loss and D. P. DiVincenzo, Phys. Rev. A **57**, 120 (1998).
[2] K. De Greve, P. L. McMahon, D. Press, T. D. Ladd, D. Bisping, C. Schneider, M. Kamp, L. Worschech, S. Höfling, A. Forchel, and Y. Yamamoto, Nat. Phys. **7**, 872 (2011).
[3] A. Greilich, S. G. Carter, D. Kim, A. S. Bracker, and D. Gammon, Nat. Photon. **5**, 702 (2011).
[4] D. Brunner, B. D. Gerardot, P. A. Dalgarno, G. Wst, K. Karrai, N. G. Stoltz, P. M. Petroff, and R. J. Warburton, Science **325**, 70 (2009).
[5] B. Eble, C. Testelin, P. Desfonds, F. Bernardot, A. Balocchi, T. Amand, A. Miard, A. Lemaître, X. Marie, and M. Chamarro, Phys. Rev. Lett. **102**, 146601 (2009).
[6] P. Fallahi, S. T. Yılmaz, and A. Imamoğlu, Phys. Rev. Lett. **105**, 257402 (2010).
[7] E. A. Chekhovich, A. B. Krysa, M. S. Skolnick, and A. I. Tartakovskii, Phys. Rev. Lett. **106**, 027402 (2011).
[8] M. Scheibner, M. F. Doty, I. V. Ponomarev, A. S. Bracker, E. A. Stinaff, V. L. Korenev, T. L. Reinecke, and D. Gammon, Phys. Rev. B **75**, 245318 (2007).
[9] K. V. Kavokin, Phys. Rev. B **64**, 075305 (2001).
[10] S. C. Bădescu, Y. B. Lyanda-Geller, and T. L. Reinecke, Phys. Rev. B **72**, 161304 (2005).
[11] S. Chutia, M. Friesen, and R. Joynt, Phys. Rev. B **73**, 241304 (2006).
[12] F. Baruffa, P. Stano, and J. Fabian, Phys. Rev. Lett. **104**, 126401 (2010).
[13] M. P. Nowak and B. Szafran, Phys. Rev. B **82**, 165316 (2010).
[14] D. Stepanenko, M. Rudner, B. I. Halperin, and D. Loss, Phys. Rev. B **85**, 075416 (2012).
[15] R. I. Dzhioev, K. V. Kavokin, V. L. Korenev, M. V. Lazarev, B. Y. Meltser, M. N. Stepanova, B. P. Zakharchenya, D. Gammon, and D. S. Katzer, Phys. Rev. B **66**, 245204 (2002).
[16] G. Burkard, D. Loss, and D. P. DiVincenzo, Phys. Rev. B **59**, 2070 (1999).
[17] G. Burkard, G. Seelig, and D. Loss, Phys. Rev. B **62**, 2581 (2000).
[18] T. Andlauer and P. Vogl, Phys. Rev. B **79**, 045307 (2009).
[19] J. Fischer and D. Loss, Phys. Rev. Lett. **105**, 266603 (2010).
[20] As a counter example, electron-hole exchange in the case of the neutral exciton is nearly Ising-like ($J\sigma_{ez}\sigma_{hz}$) with two nearly degenerate doublets separated by the exchange splitting. In that case, a small asymmetric e-h exchange $\delta(\sigma_x^h\sigma_y^e + \sigma_y^h\sigma_x^e)$ mixes the two bright excitons. Another example is the case of two holes in a single QD – one in the s-shell and the other in the p-shell. In contrast to two electrons in a single QD, the energy structure deviates strongly from isotropic, and is apparently neither Heisenberg-like nor Ising-like [33].
[21] K. V. Kavokin, Phys. Rev. B **69**, 075302 (2004).
[22] D. Kim, S. G. Carter, A. Greilich, A. S. Bracker, and D. Gammon, Nat. Phys. **7**, 223 (2011).
[23] For the hole sample we have used a Be-doped GaAs buffer, 25 nm GaAs spacer, 2.8 nm InAs bottom dot, 6 nm GaAs tunnel barrier, 3.2 nm InAs top dot, followed by 280 nm GaAs capping layer. The electron sample was

similar but with a 9 nm barrier composed of 3/3/3 nm of GaAs/$Ga_{.7}Al_{.3}As$/GaAs [22]. Both samples were covered with a 120 nm Al shadow mask perforated with one micron apertures to enable the measurement of single pairs of dots.

[24] W. G. van der Wiel, S. De Franceschi, J. M. Elzerman, T. Fujisawa, S. Tarucha, and L. P. Kouwenhoven, Rev. Mod. Phys. **75**, 1 (2002).

[25] M. F. Doty, M. Scheibner, A. S. Bracker, I. V. Ponomarev, T. L. Reinecke, and D. Gammon, Phys. Rev. B **78**, 115316 (2008).

[26] M. F. Doty, M. Scheibner, I. V. Ponomarev, E. A. Stinaff, A. S. Bracker, V. L. Korenev, T. L. Reinecke, and D. Gammon, Phys. Rev. Lett. **97**, 197202 (2006).

[27] For holes, the difference in g-factor of the InAs QDs and the GaAs tunnel barrier is substantial and $g_{12} = 0.14$ [34]. For electrons it was found that this difference was negligible with a GaAs barrier, however, it has been found recently that with a GaAs/AlGaAs/GaAs barrier, as used here, this term can also be significant ($g_{12} = 0.3$) [35]. The symmetric Hamiltonian by itself provides a good approximation to the $2e$ case.

[28] K. M. Weiss, J. M. Elzerman, Y. L. Delley, J. Miguel-Sanchez, and A. Imamoglu, (2012), arXiv:1112.4710v2 [cond-mat.mes-hall].

[29] D. Kim, S. E. Economou, S. C. Bădescu, M. Scheibner, A. S. Bracker, M. Bashkansky, T. L. Reinecke, and D. Gammon, Phys. Rev. Lett. **101**, 236804 (2008).

[30] J. M. Taylor, J. R. Petta, A. C. Johnson, A. Yacoby, C. M. Marcus, and M. D. Lukin, Phys. Rev. B **76**, 035315 (2007).

[31] We have set all γ_{ii} terms to zero at $B \sim 0$ in Eq. (4). $\Delta\gamma \gg \Sigma\gamma$ indicates that the local spin-orbit fields $\boldsymbol{\beta}_1^{so}$, $\boldsymbol{\beta}_2^{so}$ in the two QDs have opposite directions and similar magnitudes. This does not allow for any splitting between the T_0 and the T_+/T_- states, which must be less than our resolution of 15 μeV.

[32] M. F. Doty, J. I. Climente, A. Greilich, M. Yakes, A. S. Bracker, and D. Gammon, Phys. Rev. B **81**, 035308 (2010).

[33] M. Ediger, G. Bester, B. D. Gerardot, A. Badolato, P. M. Petroff, K. Karrai, A. Zunger, and R. J. Warburton, Phys. Rev. Lett. **98**, 036808 (2007).

[34] M. F. Doty, J. I. Climente, M. Korkusinski, M. Scheibner, A. S. Bracker, P. Hawrylak, and D. Gammon, Phys. Rev. Lett. **102**, 047401 (2009).

[35] W. Liu, S. Sanwlani, R. Hazbun, J. Kolodzey, A. S. Bracker, D. Gammon, and M. F. Doty, Phys. Rev. B **84**, 121304 (2011).